Contrib Mineral Petrol (1989) 103:335–345

Contributions to Mineralogy and Petrology

Mineralogy and chemistry of Cu-Fe-Ni sulfides in orogenic-type spinel peridotite bodies from Ariege (Northeastern Pyrenees, France)

J.P. Lorand

Laboratoire de Minéralogie du Museum National d'Histoire Naturelle. Unité de Recherche Associée au CNRS n° 286, 61, rue de Buffon, F-75005 Paris, France

Abstract. Mantle-derived peridotite bodies of Ariège are composed of spinel lherzolites and harzburgites ranging from remarkably fresh (less than 5% serpentinized) samples with protogranular texture to secondary foliated samples, which are generally 10%–20% serpentinized. The foliated samples have passed through two cycles of deformation and re-crystallization, the earlier ones occurring at temperatures above 950° C for 15 kbar pressure, the later ones at temperatures between 950° and 750° C for 8–15 kbar. Microscopic investigation of 140 samples reveals an accessory sulfide component which is more abundant in lherzolite than in harzburgite. This component occurs in two different textural locations, either as inclusions trapped within silicates during the first stage of re-crystallization or as interstitial grains among silicates. Mineralogy and chemistry of both sulfide occurrences are quite similar, at least in samples less than 5% serpentinized. In these "fresh" samples, sulfides are composed of complex intergrowths between nickel-rich pentlandite and pyrite, coexisting with minor primary pyrrhotite (Fe_7S_8) and chalcopyrite. Pentlandite and pyrite are interpreted as low-temperature breakdown products of upper mantle monosulfide solid solutions. The mineralogy and chemistry of interstitial sulfides in serpentinized rocks vary in parallel with the degree of serpentinization. In samples less than 10% serpentinized, primary pyrrhotite grades into FeS. In samples more than 10% serpentinized, pyrite is replaced by secondary pyrrhotite, and then disappears totally, whereas the coexisting pentlandite is Fe-enriched and replaced by mackinawite. This sequence of alteration indicates a decrease of sulfur fugacity, resulting from serpentinization of olivine at temperatures below 300° C. This is also the case for the inclusions which have been fractured during the tectonic emplacement of the host peridotites within the crust. The presence of non-equilibrium sulfide assemblages in both cases reflects the sluggishness of solid state reactions at near-surface temperatures. It is inferred from these results that sulfides disseminated within orogenic peridotite massifs are so sensitive to serpentinization that most sulfur fugacity estimates based on fractured inclusions and intergranular sulfides are unreliable.

Introduction

Although being minor phases, Cu-Fe-Ni sulfides are of great importance in mantle materials because they collect precious metals (Au and platinum-group elements) (Mitchell and Keays 1981; Garuti et al. 1984; Hamlyn and Keays 1986). Information relevant to these minerals has been drawn from ultramafic xenoliths and megacrysts in kimberlites and alkali basalts (Tsai et al. 1979; Lorand and Conquéré 1983; Pasteris 1982; Haggerty 1986; Dromgoole and Pasteris 1987; Lorand 1987; Andersen et al. 1987). In these mantle samples, present sulfide assemblages (Ni-rich pyrrhotite-like phases, pentlandite and chalcopyrite) are considered to be unmixing products of monosulfide solid solution (MSS).

Rocks equivalent to type-I spinel lherzolite xenoliths are found as km-sized bodies tectonically emplaced within the continental crust (also referred to "orogenic-type" massifs). Unlike xenoliths, the sulfide phase of these bodies has received little attention. Hitherto, the only studies available are concerned with the Ivrea Verbano zone (Baldissero, Balmuccia and Finero massifs, Italy) (Garuti et al. 1984) and the Beni-Bousera (Morocco) and Ronda (Spain) massifs (Lorand 1985). There, the subsolidus history of sulfide appears to be highly complicated by the tectonic emplacement of the host rocks within the crust, which may obliterate most of the primitive characters of the upper mantle sulfide composition (Lorand 1987). In particular, the total-metal/sulfur ratio of interstitial sulfides has increased for serpentinization degrees lower than 20% (Lorand 1985).

In the present paper, the sulfides in orogenic lherzolites are discussed for massifs from Ariège (North-eastern Pyrenees, France). The behaviour of sulfides during the incipient replacement of olivine by serpentine is documented in a suite of remarkably fresh peridotites, by comparing sulfide inclusions in silicates with interstitial sulfide grains. Once the respective subsolidus history of both sulfide occurrences is defined, sulfur fugacity estimates based on orogenic massifs are discussed.

Geological setting and petrography of the Eastern Pyrenean peridotite massifs

Peridotite massifs from Ariège outcrop as numerous small bodies (less than 1 km wide) within a small band of Mesozoïc metamorphic limestones located next to the North Pyrennean fault (Fig. 1). These massifs have been studied for more than twenty years, with respect to structure, petrology and petrogenesis of the silicate minerals (Ave Lallemant 1967; Conquéré 1971, 1977, 1978; Polvé and Allègre 1980; Loubet and Allègre 1982; Fabries and Conquéré 1983; Conquéré and Fabries 1984; Bodinier et al. 1987a, 1987b, 1988; Fabries et al. 1989). They are composed mainly of layered spinel lherzolites, with subordinate harzburgites and pyroxenites

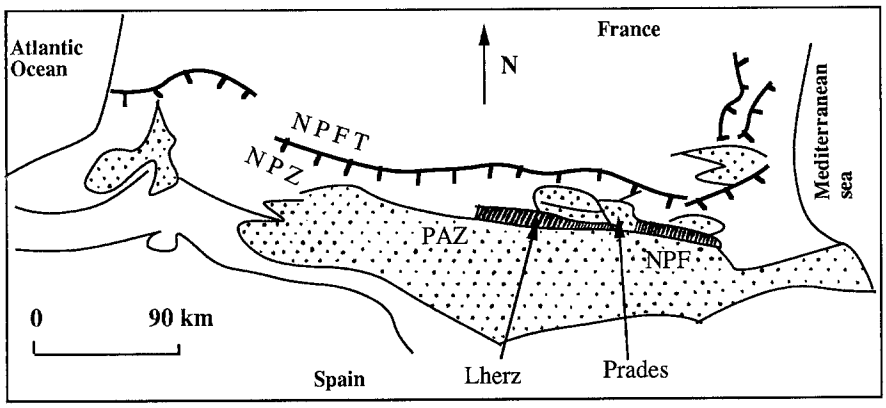

Fig. 1. Schematic geological map showing the location of the peridotite massifs from Ariège (Northeastern Pyrenees, France). *Lherz*=Lherz group (Lherz, Fontête Rouge, Freychinède, Pic Couder, Porteteny, Sem); *Prades*=Prades group (Bestiac, Caussou, Pic de Géral, Prades). Main units of the Pyrenean mountain range. *NPZ*=North Pyrenean Zone; *PAZ*=Paleozoic Axial Zone; *NPF*=North Pyrenean Fault; *NPFT*=North Pyrenean Frontal Thrust. *Dotted*=Paleozoic massifs; *hatched*=metamorphic Mesozoic terranes

(Conquéré 1978). The pyroxenites belong to two generations. The earlier one consists of spinel and/or garnet pyroxenite layers that are considered to be high-pressure, high-temperature mineral segregations from continental tholeiite melts (Conquéré 1977; Bodinier et al. 1987a). The later pyroxenite type is made of amphibole-rich pyroxenite and hornblendite dykes which cross-cut the layered rocks in the Lherz and Freychinède massifs. This pyroxenite type has been interpreted as Cretaceous alkali basalt vein-conduits (Bodinier et al. 1987b).

The peridotites represent mildly depleted partial melting residua which formed after extraction of less than 10% partial melt compositionally similar to enriched tholeiites (Bodinier et al. 1988). All the samples have been plastically deformed and underwent mantle metasomatism subsequent to the partial melting event.

The Fontête Rouge, Porteteny and Pic Couder massifs (Fig. 1) display protogranular textures which finally equilibrated between 900° and 1100° C (A. Lachmi, personal communication, 1987). In contrast, all the deformation textures observed in the other massifs are atypical according to the Mercier and Nicolas (1975) nomenclature. In fact, they result from two superimposed stages of plastic deformation and re-crystallization (Fabries and Conquéré 1983; Conquéré and Fabries 1984). The older re-crystallization is considered to postdate the asthenospheric plastic deformations. It has produced coarse-grained textures which finally equilibrated at 900°–950° C and 12–15 kbars. Olivine occurs as cm-sized poikilitic crystals enclosing orthopyroxene and spinel, and formed during a long period of steady-state subsolidus re-crystallization.

The coarse-grained texture has been preserved locally in the Sem, Bestiac and Geral occurrences. However, as a general rule, this texture grades into a high-stress, low-temperature porphyroclastic texture, especially in the Lherz massif in which ultramylonites are locally present. The prophyroclastic textures were produced by intra-lithospheric shear zones between 950° and 750° C for 8 to 15 kbar pressure (Conquéré and Fabries 1984). The secondary foliated textures are characterized by a very heterogeneous distribution of the re-crystallized matrix on thin section scale. On a larger scale, undeformed and deformed peridotites may be present within a single massif (Table 1).

Mantle metasomatism is contemporaneous with the lithospheric deformations (Vétil et al. 1988; Fabries et al. 1989). It is responsible for incompatible-trace-element enriched peridotites samples in the vicinity of amphibole-rich dykes and for titanian pargasite which is disseminated in most of the peridotites sampled away from amphibole-rich dykes. The relative modal abundance of Ti-pargasite increases from protogranular- to porphyroclastic-textured peridotites. This silicate becomes a major phase in the Caussou massif only, which has been percolated by alkali basaltic melt (Conquéré 1971; Fabries et al. 1989).

The peridotites sampled away from the periphery and faults of the massifs are exceptionally fresh (Table 1). The protogranular- and coarse-textured samples are generally less than 5% serpentinized. The porphyroclastic-textured peridotites are slightly more serpentinized, the average degree of this alteration ranging from 5%–15% in the lherzolites to 20%–30% in the harzburgites. This average degree of serpentinization may be variable within a single massif, mainly because of the textural heterogeneity of the host rock. This is especially the case at Sem, Lherz, Prades and Porteteny (Table 1). However, serpentine occurs only as mesh-textured lizardite within fracture planes and grain boundaries of olivine, a feature indicative of low-temperature and static transformations under near-surface conditions (Moody 1976).

Table 1. Main petrographic features of the peridotites from Ariège

Locality	Dominant rock type	Texture	Average degree of serpentinization[a]
Fontete rouge	lherzolite to harzburgite	protogranular	<5%
Porteteny	lherzolite	protogranular	1–8%
Pic Couder	lherzolite	protogranular	<3%
Sem	lherzolite	coarse granular to porphyroclastic	<1% 10%
Freychinède	lherzolite	porphyroclastic	5–15%
Lherz	lherzolite to harzburgite	porphyroclastic	3–15% 15–30%
Prades	lherzolite to harzburgite	coarse granular to porphyroclastic	7–30%
Géral	Cpx-rich harzburgite	coarse granular to porphyroclastic	6–16%
Caussou	lherzolite to harzburgite	coarse granular to porphyroclastic	<5%
Bestiac	lherzolite	coarse granular to porphyroclastic	1–8%

[a] Estimate from loss of ignition of whole-rock analyses (Bodinier et al. 1988; Fabriès and Conquéré 1983; Fabriès et al. 1989)

Sulfide petrography

Analytical notes

Sulfide petrology of the pyroxenites is discussed in separate papers (Lorand 1989a, b); the present study is thus concerned with the peridotites only. One hundred and forty samples, covering the range of textural and serpentinization types have been investigated on two hundred and eighty polished thin sections with respect to occurrence, textural relationships and mineral chemistry of the sulfide phases. Because sulfide grains are small (200 μm), they were studied in reflected light using high-magnifications, oil immersion objectives. Each sulfide mineral was analyzed with a fully au-

tomated CAMEBAX electron microprobe at the National Museum of Natural History (Paris), using WDS mode. Six hundred and forty spot analyses were performed on 180 sulfide grains (Table 2). Analytical error on the total metal content of the pyrrhotite is estimated to be ± 0.2 atom.% (Jover et al. 1989).

Occurrence of sulfides

Sulfides occur in all the peridotites but are more abundant in the lherzolites (50 sulfide grains per polished thin section). The sulfides have textures similar to those reported in other studies of mantle peridotites, whether xenoliths (Lorand and Conquéré 1983; Lorand 1987; Dromgoole and Pasteris 1987) or orogenic-type peridotites (Garuti et al. 1984; Lorand 1985, 1987). They occur either as interstitial grains or as inclusions within the major phases. Interstitial sulfides, i.e. sulfides situated between grains of silicates and spinel, account for a major proportion of the total sulfide in all of the peridotites: however, abundance, shape and size of both the enclosed and the interstitial sulfides vary according to the deformation texture of the host rock.

Three types of enclosed sulfide can be distinguished: (1) trails of sulfide inclusions associated with fluid-inclusion arrays, (2) tubular or cylindrical bodies aligned along parallel cleavage planes of pyroxenes, (3) isolated sulfide inclusions. The first type is present in all the peridotite sub-types and displays all the characteristic features of secondary inclusions (Roedder 1984). The trails consist of small sulfide blebs interspersed with fluid inclusions displaying negative crystal shapes. These trails of inclusions cross-cut the grain or sub-grain boundaries of silicates without a marked change in direction. The second type of sulfide inclusion is preferentially distributed in the protogranular peridotites, especially in the pyroxenes associated with Al-Cr spinel.

The third type of sulfide inclusion (i.e. isolated sulfide inclusion) is not preferentially associated with fluid inclusion arrays nor with cleavage, parting or fracture planes in their host silicate. It consists of single blebs much larger than the sulfides in secondary inclusion arrays. These blebs are found in coarse and porphyroclastic samples. Two or three inclusions per polished thin section is a common average value in all the samples but those from Bestiac may contain up to 10 inclusions in a single polished thin section. These inclusions occur in all silicates but most commonly in olivine (67%) and orthopyroxene (24%). They are virtually absent from spinel. Commonly, isolated sulfide inclusions have round or oval cross sections with dimensions exceeding 50 μm (Fig. 2A); elongated inclusions occur in pyroxenes.

Isolated sulfide inclusions have been interpreted as sulfide incorporated during secondary grain growth of olivine and pyroxenes in the upper mantle (Lorand 1987). The trapping process would be similar to the one producing inclusions of spinel in re-crystallized olivine (Mercier and Nicolas 1975). This is supported by the specific location of isolated sulfide inclusions in recrystallized peridotites. Moreover, several intermediate stages of sulfide incorporation are observed within a single thin section as round interstitial grains partly engulfed within olivine. Also, isolated inclusions are especially abundant in the peridotites close to amphibole-rich dykes, a feature which may be explained by the fact that H_2O pressure enhances silicate grain boundary migration during subsolidus re-crystallization (Cordellier 1982).

Many isolated inclusions are surrounded by fracture planes radiating out from the central inclusions (Fig. 2B). Some of these fractures reach the host crystal margins. Similar fractured sulfide inclusions are common in clinopyroxene megacrysts and in ultramafic xenoliths from alkali basalts (Andersen et al. 1987; Dromgoole and Pasteris 1987; Lorand 1987). Generally, in these mantle materials, the central sulfide inclusions have stellate or decorated borders; moreover the fracture planes contain satellite sulfide inclusions interspersed with CO_2-rich fluid inclusions. Such features have been ascribed to melting and expansion of the sulfide, probably enhanced by explosive boiling of CO_2, during the ascent and decompression of the xenoliths (Dromgoole and Pasteris 1987; Andersen et al. 1987). Unlike these xenoliths, fractured sulfide inclusions in the Eastern Pyrenean peridotites have smooth grain boundaries and are devoid of satellite sulfide or fluid inclusions, probably because the decompression was much slower and occurred without sulfide remelting.

Interstitial sulfides are anhedral and not round like the inclusions (Fig. 2C to H). They display curvilinear margins moulded around silicates reflecting solidification of immiscible sulfide liquids (Garuti et al. 1984; Lorand 1987). In the protogranular peridotites, the majority of the interstitial sulfides are 0.2 mm-wide blebs adjacent to pyroxene-spinel clusters. This sulfide type has dimensions up to 2 mm in the Sem coarse-grained peridotites. On the other hand, the prophyroclastic peridotites contain two populations of sulfide grains. Large sulfide grains persist in parts of the rock which escaped lithospheric shearing deformations. The microgranular re-crystallized matrix contains only small sulfide grains (less than 100 μm wide), which obviously resulted from brecciation of larger sulfide grains. These grains show features of textural equilibrium with the silicate phases such as 120° triple junctions.

Sulfide inclusions

The sulfide inclusions are composed of pentlandite (Pn), pyrite (Py), chalcopyrite (Cp) and pyrrhotite (Po), without primary magnetite. Modal proportions of sulfide phases vary widely between aggregates due to non-uniform phase distribution. Monomineralic Pn grains are rare. Many sulfide inclusions are Pn + Py + Cp three-phase assemblages. Po, Py and Cp are always associated with pentlandite. Pn is however predominant, except near pyroxenite layers and dykes.

In upper mantle rocks as well as in crustal basic and ultrabasic rocks, the Pn + Po + Cp assemblage is considered to be an unmixing product of high-temperature monosulfide solid solutions (MSS) (Kullerud et al. 1969; Craig and Kullerud 1969). Thus, its constitutive sulfides are usually labeled "primary" with respect to low-temperature alteration products (serpentinization and supergene weathering) (Garuti et al. 1984; Lorand 1987). Pn, Po and Cp are undoubtly primary in the Eastern Pyrenean peridotites since they are constantly enclosed in silicates. Py has been interpreted as primary by Babkine et al. (1966) and Conquéré (1978), but of late origin by Besson (1975). Typically, Py is intergrown with Pn whereas Po and Cp form discrete masses near the edges of the sulfide inclusions (Fig. 2A). This textural feature, together with its Co-rich character (Table 2) suggest that Py is contemporaneous with Pn, and therefore, primary (e.g. Ewers and Hudson 1972).

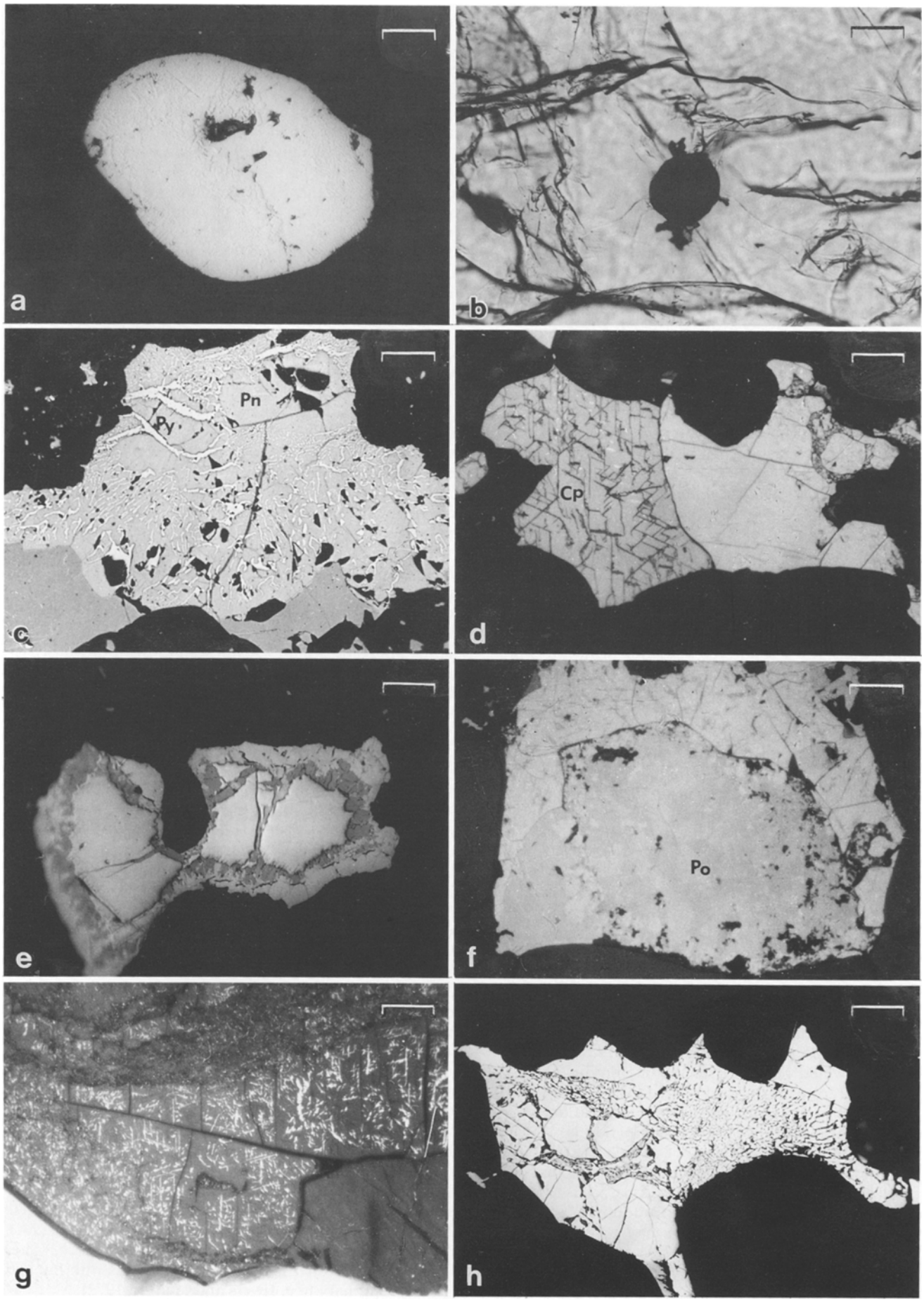
a
b
Pn
Py
c
Cp
d
e
Po
f
g
h

Table 2. Representative electron microprobe analyses of individual sulfides included in silicates and some MSS compositions

Mineral (wt %)	Int.	MSS1	MSS2	Pn	Py	Po	Cp	Pn	Po	Po
Fe	34.4	36.2	35.5	29.1	45.1	58.8	30.0	34.7	61.6	62.2
Ni	25.5	24.7	22.9	36.7	0.5	1.1	0.2	32.2	0.1	0.4
Co	0.5	0.3	0.8	0.4	1.8	–	–	0.4	–	–
Cu	–	0.1	0.6	–	–	–	34.2	–	0.1	–
S	38.9	38.8	38.5	33.7	52.8	39.7	35.2	33.0	38.8	36.2
Total	99.3	100.1	98.3	99.9	100.2	99.6	99.6	100.3	100.6	98.8
Atomic ratio										
Fe/Ni	1.41	1.51	1.63	0.83	–	–	–	1.13	–	–
Cu/Fe	–	–	–	–	–	–	1.00	–	–	–
Fe/S	–	–	–	–	–	0.86	–	–	0.91	0.99
								F	F	F

Int. = Analysis of symplectite-like intergrowths between Pn and Py, using broad-beam techniques. *MSS1* = Representative analysis of monosulfide solid solution from spinel lherzolite xenoliths of the French Massif Central alkali basalts (Lorand and Conquéré 1983); *MSS2* = monosulfide solid solution synthesized at 500° by heating Pn + Py + Po + Cp ores (McQueen 1979). *F* = fractured inclusion; *Pn* = pentlandite; *Py* = pyrite; *Po* = pyrrhotite; *Cp* = chalcopyrite. Analytical conditions: acceleration voltage: 15 kV; counting time: 6s:peak, 6s:background; specimen current: 10 nA. Pure metal standards except for Fe and S (natural pyrite). –, below detection (0.05 wt %)

The composition of intergrowths between Pn and Py have been determined by electron microprobe using a 20 μm-defocussed electron beam. In spite of poor accuracy of such a procedure (loss of correction for fluorescence and absorbtion coefficients; Reed 1975), most of the bulk analyses (Table 2) plot within the compositional limits of MSS at 600° C (Fig. 3). The bulk compositions are also similar to MSS from spinel lherzolite xenoliths in alkali basalts (Lorand and Conquéré 1983; Dromgoole and Pasteris 1987) or to MSS experimentally produced by heating Po + Pn + Py + Cp ores at 500° C (McQueen 1979) (Table 2). All these compositional similarities argue for an hypothesis of simultaneous exsolution of Pn and Py from Ni-rich MSS.

Pn and Po display a wide range of compositions with respect to Ni/Fe and base metal/sulfur ratio, but have Cu concentrations of less than 0.1 wt%. In fact, their compositions depend on whether the inclusions were fractured during emplacement within the crust or not. The unfractured inclusions contain Ni-rich Pn (Fig. 3). The total-metal/sulfur ratio of the Po is close to 0.87 despite some spread in the values (Fig. 4); the Ni concentrations are low (0.1–1 wt%) (Table 2). Cp is slightly Cu-deficient with respect to stoichiometric $CuFeS_2$, in agreement with its presence in Po and Py-bearing sulfide assemblages (Fig. 5).

In fractured inclusions, the total-metal/sulfur of the Po ranges from 0.90 to 1.0, in some case approaching troilite in composition (Tr) (Fig. 4). Ni rarely exceeds 0.5 wt%. The Pn contains less than 33 wt% Ni (Figs. 3–6). The relation between the Ni content of the Pn and the total-metal/sulfur of the Po is similar to that previously found in experimental as well as in natural Fe-Ni-S ores (Graterol and Naldrett 1971; Misra and Fleet 1973) (Fig. 5). In addition to this decreasing Ni content, Pn is replaced by randomly orientated 10 μm-thick mackinawite (Mw) blebs.

Interstitial sulfides

Interstitial sulfides are composed dominantly of the same primary phases as the inclusions. Pn predominates over the other sulfides except in peridotites next to pyroxenitic bands and dykes where Po is more abundant. The primary sulfides are partly altered into iron hydroxides and secondary sulfides. This alteration, which is more pronounced in the massifs of Bestiac, Caussou, Pic de Calmont and Porteteny, develops the typical features of supergene weathering (Watmuff 1974): Py, Pn and Cp are transformed into iron hydroxides, millerite (Mi), violarite (Vi), bravoite (Bv), covellite (Cv), chalcocite (Cc) and bornite (Bo), respectively. In some cases, smythite (Fe_9S_{11}) is observed along edges or cleavage planes of Po, which becomes greyish-white in

Fig. 2A–H. Photomicrographs illustrating sulfide types. **A** Isolated sulfide inclusion in olivine (dark) containing symplectite-like intergrowth between pentlandite (*Pn*) and pyrite (*Py*). Lherzolite from Bestiac. Plane polarised reflected light, oil immersion. Scale bar = 10 μm; **B** Fractured sulfide inclusion (dark) in olivine. Note cracks radiating out from the sulfide inclusion. Lherzolite from Bestiac. Plane polarised transmitted light. Scale bar = 50 μm; **C** Large interstitial sulfide grains displaying symplectite-like intergrowth between Pn and Py together with primary pyrrhotite (*Po*) (medium grey). Lherzolite from Bestiac. Plane polarised reflected light, oil immersion. Scale bar = 100 μm; **D** Two-phase interstitial sulfide grain composed of pentlandite (light grey) and discrete chalcopyrite (*Cp*); Lherzolite from Lherz. Plane polarized reflected light, oil immersion. Scale bar = 50 μm; **E** discrete Py (white) included within interstitial Pn (medium grey). Note the rim of secondary Po (dark grey) around the Py. Lherzolite from Sem; plane polarized reflected light, oil immersion. Scale bar = 50 μm; **F** Discrete Py totally replaced by polycrystalline secondary Po (medium grey) adjacent to Pn (light grey). Lherzolite from Lherz. Plane polarised reflected light, oil immersion. Scale bar = 50 μm; **G** Interstitial Pn (dark) replaced by mackinawite blebs (white) along fracture and cleavage planes. Lherzolite from Freychinède. Crossed-polarised reflected light, oil immersion. Scale bar = 20 μm; **H** Monomineralic grain of Pn interstitial to silicate. Note the symplectites filled by PoII. Lherzolite from Lherz. Plane polarised reflected light, oil immersion. Scale bar = 50 μm

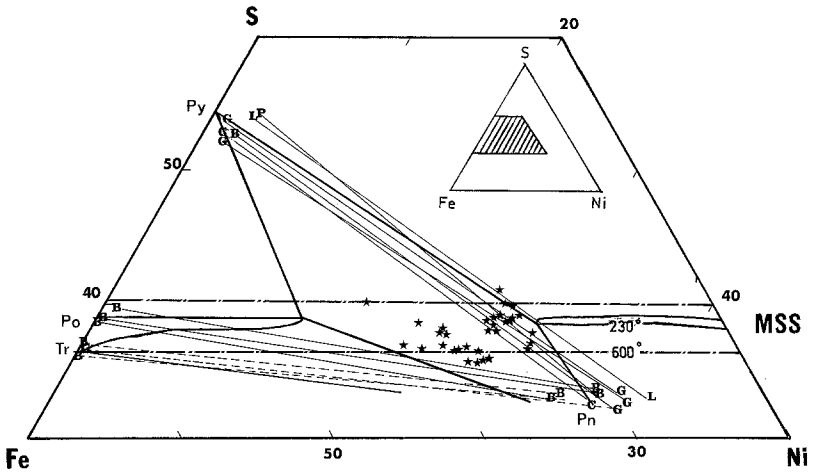

Fig. 3. Compositions of individual sulfide minerals included within silicates plotted on Fe-Ni-S ternary (wt %). Key to symbols, *B* = Bestiac; *G* = Geral; *C* = Caussou; *P* = Prades; *L* = Lherz; stars = defocussed-beam microprobe analyses of intergrowths between pentlandite and pyrite; *dashed tie-lines* = sulfide assemblages from fractured inclusions; *dashed-dotted lines* = compositional limits of MSS at 600° C (Naldrett et al. 1967); *heavy lines* = enlarged portion of the Fe-Ni-S system at 230° C (Craig 1973; Misra and Fleet 1973). *MSS* = monosulfide solid solution; *Py* = pyrite; *Po* = pyrrhotite; *Tr* = troilite; *Pn* = pentlandite

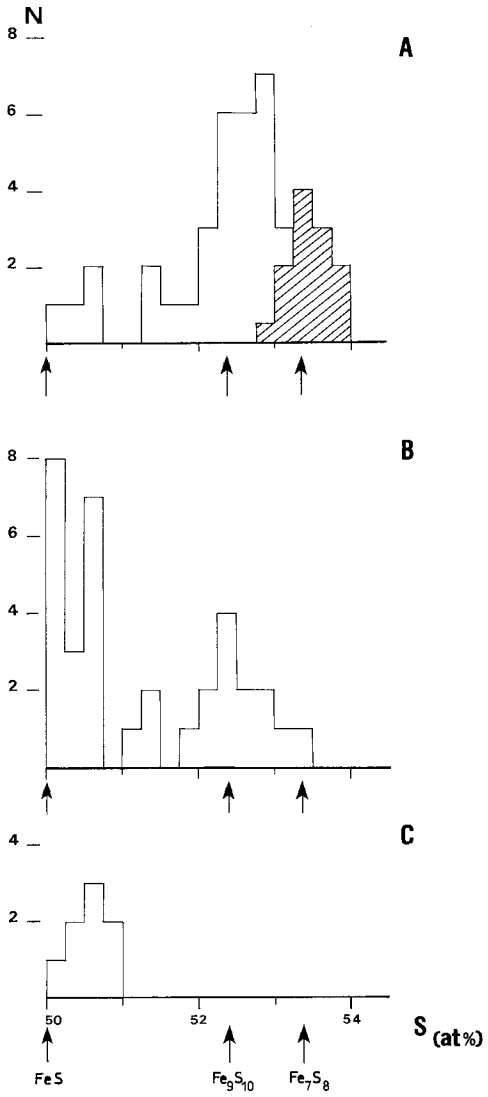

Fig. 4A–C. Histograms showing compositional ranges (at 0.25 at% intervals) of primary pyrrhotite (Po I) in terms of atomic percent sulfur. **A** sulfide inclusions; **B** interstitial pyrrhotite from Bestiac; **C** interstitial pyrrhotite from Lherz, Freychinède and Sem. *FeS* = troilite; Fe_9S_{10} = hexagonal-type pyrrhotite; Fe_7S_8 = monoclinic-type pyrrhotite; *shaded area* = unfractured inclusions; *N* = number of grains analysed

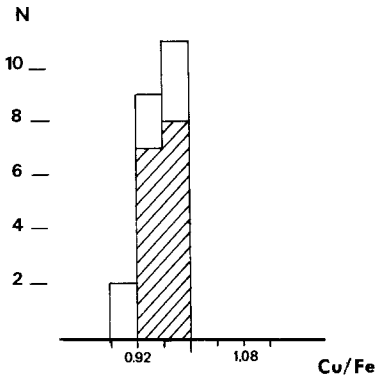

Fig. 5. Histogram showing compositional range of chalcopyrite in terms of Cu/Fe atomic ratio. *Shaded area* = chalcopyrite included in silicate; *open area* = chalcopyrite interstitial to silicate; *N* = number of grains analysed

reflected light. The grains containing one or more supergene alteration products have been discarded from microprobe analyses.

There is a general relationship between mineralogy and mineral chemistry of the interstitial sulfides and the degree of serpentinization of the host samples. This relation is revealed only by comparing the interstitial sulfide assemblages with the coexisting silicate-hosted sulfide inclusions.

The interstitial sulfides from the least serpentinized samples (i.e. Pic Couder, Caussou, Bestiac, Sem, Freychinède) are compositionally very similar to the coexisting inclusions. Sulfides form various two-, three- or four-phase assemblages but Pn, Cp and Po may occur as monomineralic grains. Co-rich pyrite is present in most of the sulfide grains, and in some cases, exceeds 50 vol.%. Py is always associated with Pn with which it forms symplectite-like intergrowths (Fig. 2C). The compositions of these intergrowths analysed by broad-beam techniques plot within the MSS field in the Fe-Ni-S system (Fig. 7). Less commonly (Caussou and Sem samples) Pn contains large, round inclusions of Py (Fig. 2E), which indicates that, in some cases, Py has crystallized before Pn.

Pentlandite in the Pn-Py-Po-Cp bearing assemblages is fairly homogeneous with Fe/Ni ratio lower than 1 (Fig. 6B). Exsolution intergrowths of Cp in Pn and vice

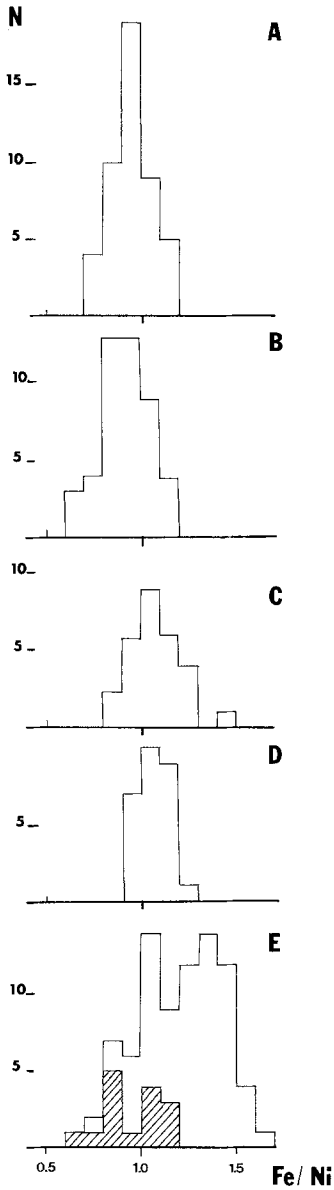

Fig. 6A–E. Histograms showing compositional ranges of pentlandite in terms of Fe/Ni atomic ratio. **A** = sulfide inclusions; **B** = Pn-Py-Po-Cp interstitial sulfide assemblage; **C** = Pn-Py-PoII-Cp interstitial sulfide assemblages; **D** = Pn-PoII-Mw-Cp interstitial sulfide assemblages; **E** = Pn-Tr-Cp-Mw interstitial sulfide assemblages. For abbreviations of mineral names, see text. *Shaded area* = samples in which relicts of Py have been observed; *N* = number of grains analysed

versa are frequent, as previously reported in intracontinental lherzolite massifs (Garuti et al. 1984; Lorand 1985). Unlike the other primary sulfides, Po exhibits compositional differences with respect to Po from unfractured sulfide inclusions. Ratios of total-metal/sulfur range from 0.9 to 1.0 (Fig. 4B). The Ni and Cu concentrations are respectively close to or below the detection limits of the analytical procedure; these decreasing Ni and Cu contents are coupled with exsolution of Pn and Cp lamellae and flames in the Po.

In samples more than 5%–10% serpentinized, Py becomes much less abundant and is replaced by polycrystalline pyrrhotite (PoII) ranging in composition from monoclinic pyrrhotite to troïlite (Table 3). The replacement of Py by PoII is highly non-uniform. For instance, within a single thin section, some grains of Py are surrounded by a thin rim of PoII (Fig. 2E) whereas others, a few hundred micrometres apart, are fully pseudomorphed (Fig. 2F). Generally, the breakdown of Py is accompanied by crystallization of abundant nickeliferous Mw blebs in Pn (Fig. 2G).

In samples containing more than 20 wt% serpentine, the interstitial sulfide assemblages are devoid of Py and PoII although, in a single thin section, Py may be present in sulfide inclusions isolated within silicates. Pn occurs as discrete homogeneous masses associated with Cp and (or) Po (Fig. 2D), or as grains in which vermicular holes form networks looking like Py habits (Fig. 2H). Microprobe analyses reveal strong Co-enrichments at the margins of these holes, a feature which suggests that they could have formed from complete dissolution of Py during serpentinization.

The composition of Po in Py-poor samples is fairly homogeneous (total-metal/sulfur ratio near 1 in Fig. 4C). Pentlandite exhibits a wide range of Fe/Ni ratios (Fig. 6C, D, E). However, the correlation between the Fe/Ni ratio in Pn and the coexisting sulfide assemblages (Misra and Fleet 1973) is not always evident. For instance, pentlandite coexisting with troïlite or secondary pyrrhotite may exhibit the same Fe/Ni ratio as grains associated with pyrite. In a single pentlandite grain, Fe content commonly increases towards grain edges (Table 3). All these within-grain and between-grain variations are responsible for the bimodal distribution of the histogram in Fig. 6E.

Discussion

Crystallization and subsolidus history of the unfractured sulfide inclusions

Sulfides in the Eastern Pyrenean peridotites are considered to have formed from an immiscible sulfide liquid partly trapped after partial melting (Lorand 1989c). This interpretation is consistent with several textural criteria. First, the close association between sulfides and pyroxene + spinel clusters in protogranular peridotites, the isolated sulfide inclusions in olivine and pyroxenes, and the two classes of interstitial sulfides all indicate that sulfides were present prior to deformation and re-crystallization which occurred in the mantle. Second, the isolated sulfide inclusions have the typical geometry of immiscible sulfide liquid with minimum surface. Third, equilibrium textures such as 120° triple junctions between sulfide grains and adjacent silicate phases are observed, suggesting thermal recrystallization.

The crystallization history of this sulfide liquid, and the subsolidus changes which occurred to produce the present sulfide mineralogy, are generally estimated from experimental studies on phase relationships in the Cu-Fe-Ni-S quaternary system. Since the phase relationships are very sensitive to small changes in total-metal/sulfur bulk ratio (Craig and Kullerud 1969; Kullerud et al. 1969), the cooling history of the sulfide component can be assessed only if it occurred without large change in sulfur fugacity. Strictly speaking, the data presented before and the discussion below indicate that this condition was fulfilled in the inclusions only.

For sulfide assemblages dominated by Pn + Py + Po, such as those included in silicates, MSS compositions are inevitable at mantle depths (Kullerud et al. 1969). The MSS can contain about 7 wt % Cu at 935° C which is exsolved at lower temperature as intermediate solid solution (ISS),

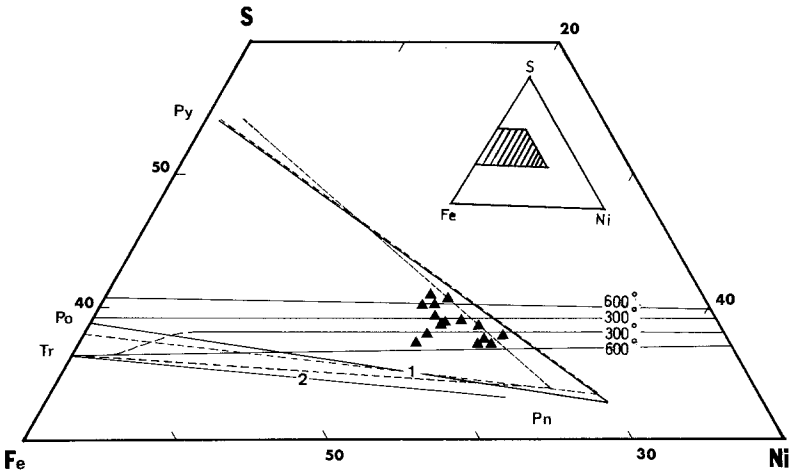

Fig. 7. Composition of interstitial intergrowths between Pn and Py (full triangles) and of main interstitial sulfide assemblages plotted on Fe-Ni-S ternary (wt %). *1* = Pn-Py-Po assemblage from samples less than 5% serpentinized; *2* = Pn-Tr assemblage; *dashed lines* = Pn-Py-Tr nonequilibrium assemblages. Compositional limits of MSS at 300 and 600° C after Naldrett et al. (1967). Other symbols as in Fig. 3

Table 3. Representative electron microprobe analyses of individual integranular sulfides

Mineral locality (wt %)	Inter B	Pn B	Py B	PoII B	PoII B	Cp B	Pn S	Pn B	Tr L	Pn L	PnII L	PoII S	PoII S	Mw L
Fe	36.4	30.5	45.1	59.1	60.5	21.7	29.5	33.3	63.2	39.4	37.3	61.2	63.2	40.4
Ni	26.0	37.0	0.6	0.4	0.4	0.1	42.4	32.7	–	25.8	29.4	0.2	0.3	22.7
Co	0.6	0.2	1.2	–	–	–	0.3	0.3	0.1	0.3	–	–	–	–
Cu	0.2	–	–	0.1	–	33.2	–	–	–	–	–	–	–	0.1
S	36.2	32.9	53.5	39.2	38.6	34.7	32.9	33.1	36.4	34.0	33.2	39.1	37.1	35.1
Total	99.4	100.6	100.4	98.8	99.5	99.7	100.1	99.4	99.7	99.5	99.9	100.5	100.6	98.3
Atomic ratios														
Fe/Ni	1.47	0.86	–	–	–	–	0.58	1.98	–	1.60	1.33	–	–	2.00
Cu/Fe	–	–	–	–	–	0.92	–	–	–	–	–	–	–	–
Fe/S	–	–	–	0.87	0.90	–	–	–	0.99	–	–	0.90	0.98	–

Int. = analysis of symplectite-like intergrowth between Pn and Py using broad-beam techniques; *Pn* = pentlandite; *Py* = pyrite; *PoI* = primary pyrrhotite; *Cp* = chalcopyrite; *Tr* = troilite; *PnII* = flame-like exsolution of pentlandite in PoI; *PoII* = secondary pyrrhotite; *Mw* = mackinawite; *B* = Bestiac; *S* = Sem; *L* = Lherz

the high-temperature precursor of chalcopyrite and cubanite (Cabri 1973). The occurrence of monomineralic grains of Cp however suggests that all of the ISS did not exsolve from MSS but rather formed from a Cu-rich sulfide liquid.

The chemical similarities between MSS from spinel lherzolite xenoliths and the bulk compositions of Pyrenean pentlandite-pyrite intergrowths suggest that crystallization temperatures and subsolidus history were similar in both cases. An MSS containing 38.5 wt % sulfur and with Ni/Ni+Fe ratio of 0.386, i.e. close to the average values of pentlandite+pyrite defocussed-beam analyses, would start to crystallize at about 1070° C from the sulfide liquid (Lorand and Conquéré 1983). Although the pressure effect on the stability temperature of Cu-Fe-Ni sulfides is poorly constrained, the temperature of the first crystallization of MSS is expected to increase up to 1150° C for 15 kbar pressure (Ryzhenko and Kennedy 1973). On the other hand, this temperature could have been lowered to some extent if other fluid species such as O_2 and CO_2 were dissolved in the sulfide liquid (Naldrett 1969; Andersen et al. 1987). The lack of primary magnetite intergrown with sulfide and the absence of two-phase CO_2-sulfide inclusions suggest that we are dealing with a nearly pure sulfide component. The reason for that is unclear. At least for O_2, Naldrett (1969) argued that if pyrrhotite is the first crystallizing phase, then a molten sulfide should lose all of its oxygen if fO_2 and fS_2 are buffered by the surrounding alumino-silicate magma. Another likely controlling factor is pressure which greatly reduces the solubility of oxygen in sulfide melt (Wendlandt 1982).

The ISS could crystallize from a Cu-rich liquid at a temperature of about 900° C (Dutrizac 1976). It can contain 15 wt % Ni at 700° C (Craig and Kullerud 1969) but the Ni solubility is reduced to 2 wt % at 500° C (McQueen 1979). The very low Ni concentration and Pn exsolution lamellae in Cp suggest that subsolidus re-equilibration continued to a very low temperature. This temperature can be better estimated by looking at the Fe-Ni-S system. At temperatures from about 1150° C down to below 300° C, the Fe-Ni sulfides would have existed as a single MSS (Figs. 3 and 6). At 250° C, the MSS compositional field is interrupted by a solvus, which makes the simultaneous crystallization of Pn and Py possible (Fig. 3) (Misra and Fleet 1973; Craig 1973). Below 250° C, the sulfide would have consisted of Mss1 + Pn + Py. At this temperature, the solubility of Ni within Mss1 is about 18 at % so that Pn and monoclinic Po cannot coexist stably (Misra and Fleet 1973). Given the presence of this mineral pair in the unfrac-

tured inclusions, the maximum blocking temperature of subsolidus reequilibration is estimated to be much lower than 250° C.

This temperature is more likely to be close to a few tens of degrees, because most of the inclusions contain low-Ni pyrrhotite. By comparison, the blocking temperatures of sulfides in alkali basalt-hosted peridotite xenoliths range between 200° and 300° C (Lorand and Conquéré 1983; Dromgoole and Pasteris 1987). Although not large, this difference of blocking temperature accounts for the difference in sulfide mineralogy between the two sulfides occurrences; in fact, experimental phase diagrams in the Fe-Ni-S system show that, for a single bulk sulfide composition, a T decrease of 200° C is large enough to produce Pn + Py + Po assemblages instead of the MSS-dominated sulfides which characterize ultramafic xenoliths from alkali lavas (Lorand 1987) (Figs. 3 and 7).

The compositional similarities between enclosed and interstitial sulfides from the least serpentinized samples suggest that both sulfide types underwent the same crystallization and subsolidus history. However, pyrite crystallizes prior to pentlandite in the samples of Sem and Caussou. Theoretically, Py is unstable above 810° C at 5 kbar pressure, where it reacts to pyrrhotite and sulfur (Kullerud and Yoder 1959). It seems unlikely for Py to have crystallized at such a high temperature for several reasons. First, it should have required sulfur in excess with respect to MSS compositions (Kullerud et al. 1969), which in return requires unusually high sulfur fugacity. Second, sulfur should have reacted with olivine to form additional pyrite apart from pentlandite (Kullerud and Yoder 1963) for which there is no textural evidence. Third, although early crystallized, Py is constantly associated with Pn, which suggests exsolution from MSS. The exsolution of Py prior to Pn is possible in the temperature range 600–300° C, provided that the sulfide bulk compositions plot on the sulfur-rich boundary of the MSS field (Fig. 7); after exsolution of Py, the sulfide bulk composition would have moved towards the metal-rich boundaries of the MSS, which would allow the exsolution of Pn. Py, Cp and MSS can coexist stably at 334° C in the pure Cu-Fe-S system but this temperature reaches 425° C for Ni concentrations of 10 wt % (Craig and Kullerud 1969) and, possibly, higher temperatures for Pn-rich samples.

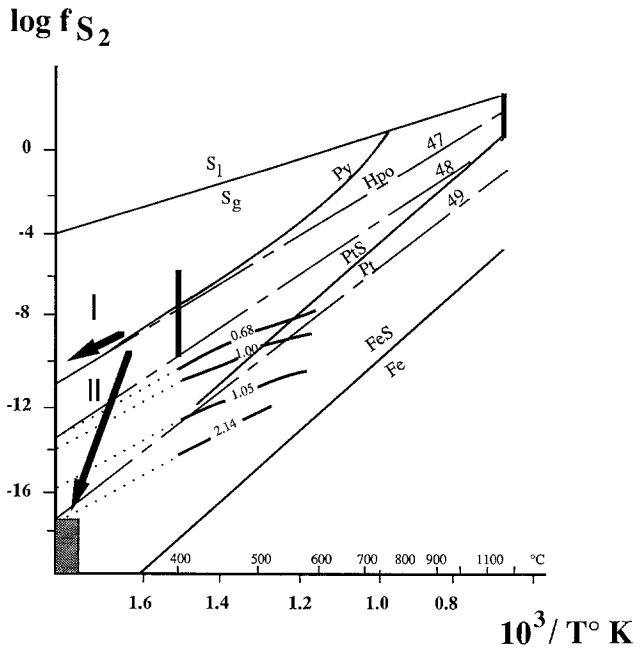

Fig. 8. Sulfur fugacity estimates as deduced from the unfractured inclusions (*vertical bar*) and from the fractured inclusions and interstitial sulfides (*shaded area*). *Thick lines* = Fe:Ni atomic ratio of pentlandite experimentally studied by Kaneda et al. (1986); *dashed lines* = composition of Po in terms of atomic percent iron (Toulmin and Barton 1964); *Fe:* native iron; *FeS:* troilite; *Hpo:* hexagonal pyrrhotite; *Py:* pyrite; S_g: gaseous sulfur; S_l: liquid sulfur (after Vaughan and Craig 1978). PtS-Pt buffer curve after Stockman and Hlava (1984). *Arrow* = subsolidus re-equilibration paths (I: unfractured inclusions; II: fractured inclusions and interstitial sulfide grains)

The effect of serpentinization

The exsolution of Py prior to Pn and the co-stability of Py and Cp are both indicative of sulfur fugacity higher than 10^{-8} atm. at 400° C (Barton 1973). Ni-rich Pn is stable at higher sulfur fugacities than the Fe-rich end-members (Kaneda et al. 1986). Accordingly, the disappearance of Py, the increasing Fe/Ni ratio of Pn, the troïlite composition of Po, all indicate that the final equilibration of the interstitial sulfides occurred under lower fS_2 conditions than for the unfractured inclusions (Fig. 8). This conclusion is also valid for the fractured inclusions since they contain troïlite-type Po coexisting with Fe-rich Pn. Given the mineralogical evidence, namely the covariance between the sequence of alteration of sulfides and the degree of serpentinization of the host rocks, this decrease of fS_2 is attributed to reactions with low-temperature serpentinizing fluids.

This interpretation is supported by temperature estimates for sulfide alteration reactions. First, assuming that crystallization temperature estimates for Py are correct, the replacement of this sulfide by PoII should have occurred below 600° C, if Py has crystallized before Pn, and most likely below 250° C if Py was initially intergrown with Pn. Second, the breakdown of Py into PoII is balanced by the replacement of Pn by mackinawite. Although there is uncertainty about the stability of mackinawite, this phase is generally considered to be stable at temperatures below 200° C (see Takeno et al. 1982 and Lorand 1985). Such low temperatures are consistent with those commonly assumed for retrograde serpentinization of olivine in a static environment (Moody 1976). Moreover, the reactions involving both the fractured inclusions and the interstitial sulfides are far from completed. Py and FeS-type pyrrhotite cannot coexist stably at any temperature in the Fe-Ni-S system; likewise, the core-rim zoning and the bimodal distribution of Fe/Ni ratios of Pn is indicative of incomplete equilibration of FeS-bearing sulfide assemblages in terms of fS_2 (Fig. 8). The persistence of Py in sulfide assemblages which have experienced serpentinization is probably due to its highly non-reactive nature at low temperature (Yund and Hall 1970).

The increase of the total metal to sulfur ratio in sulfides is generally ascribed to reactions with H_2-rich reducing fluids generated by serpentinization which liberates sulfur as H_2S (Eckstrand 1975). In the Ariège peridotites, several processes may be inferred in order to account for the present intergranular sulfide assemblages. These processes are strongly dependent upon the initial metal-to-sulfur ratio of each sulfide grain and the temperature of serpentinization. For instance, it can be assumed that some bulk sulfide

compositions plot within the MSS compositions at 300° C. Isochemical cooling would have produced the intergrowths between Pn and Py at 250° C (Fig. 7). Serpentinization occurring below this temperature would have caused the replacement of the Py by secondary pyrrhotite according to the reaction

$$7\ FeS_2 + 6H_2 \rightleftharpoons Fe_7S_8 + 6H_2S$$

In contrast, at temperature above 300° C, the same reaction would have involved MSS instead of Py. By reacting out with the H_2-rich fluids, the MSS would have liberated sulfur so that its composition shifted towards the pentlandite solvus, making crystallisation of pyrite impossible (Fig. 7). This latter case pertains to intergranular assemblages free of pyrite or secondary pyrrhotite. Some of the heterogeneity in sulfide mineralogy may therefore be explained by slight differences in serpentinization temperatures; it is unlikely that the front of serpentinization progressed at a constant temperature in the whole ultramafic mass.

Mackinawite is easily formed from H_2S-rich aqueous fluids (Takeno et al. 1982). An interstitial aqueous phase, capable of dissolving metals and sulfur, would also facilitate rapid and thorough subsolidus re-equilibration of the sulfide phase (McQueen 1979). This is probably the reason why flame-like exsolution bodies of pentlandite occur in the intergranular pyrrhotite but not in the pyrrhotite included in silicates. Such flames form below 150° C by homogeneous nucleation of orientated lamellae from the residual Ni still held in solid solution within MSS (Kelly and Vaughan 1983).

Conclusion

Intergranular sulfides and fractured sulfide inclusions display incipient replacement features in fresh peridotites containing only trace amounts of serpentine. These results are strongly consistent with earlier works concerned with peridotite massifs tectonically emplaced within the continental crust. The first stage of alteration is always marked by the crystallization of sulfur-deficient sulfides such as FeS-type pyrrhotite and mackinawite. This stage, which precedes the transformation of sulfides into native metals (e.g. Lorand 1985) has to be integrated in general models for sulfide alterations during serpentinization, especially since it has also been recognized in mafic igneous complexes (Papunen 1970; McQueen 1981).

Because serpentinization increases the total-metal/sulfur ratio, isochemical or nearly isochemical subsolidus re-equilibration cannot be invoked for the intergranular sulfide component and fractured inclusions. Most sulfur fugacity values based on these sulfide occurrences are probably unreliable. For example, starting from the interstitial FeS-type pyrrhotite, Besson (1975) has estimated the fugacity of sulfur in the Eastern Pyrenean peridotites to be 10^{-3} to 10^{-6} atm. at 1100° C. Considering the unfractured inclusions, the simultaneous crystallization of pyrite and pentlandite or chalcopyrite, the total-metal/sulfur ratio of the Po, the Fe/Ni ratio of Pn, all indicate $\log fS_2$ values ranging between -7 and -10 at 400° C (Craig and Naldrett 1968; Barton 1973; Kaneda et al. 1986) (Fig. 8). Extrapolation at constant metal/sulfur ratio leads to $\log fS_2$ values in the range -1 to $+1$ in the mantle source of the Eastern Pyrenean peridotites, i.e. several log units higher than postulated by Besson (1975).

Acknowledgements. Thanks are due to Drs. J. Fabries, M. Guiraud, Z. Johan and A.J. Naldrett for helpful discussions. I wish also to thank R.A. Binns for editorial comments and D.R. Hudson and an anonymous reviewer for their critical reading of the manuscript. This work was financially supported by the "Centre National de la Recherche Scientifique". Grant n° 983030 (ATP Microphases).

References

Andersen T, Griffin WL, O'Reilly SY (1987) Primary sulphide melt inclusions in mantle-derived megacrysts and pyroxenites. Lithos 20:279–295

Ave Lallemant HG (1967) Structural and petrographic analysis of an "Alpine-type" peridotite: the lherzolite of the French Pyrenées. Leidse Geol Mededel 42:1–57

Babkine J, Conquéré F, Vilminot JC (1966) Note préliminaire sur les minéraux opaques dans les roches ultrabasiques des Pyrénées. CR Acad Sci Paris Ser II:453–455

Barton PB (1973) Solid solutions in the Cu-Fe-S system. Part1. The Cu-S and the Cu-Fe-S joins. Econ Geol 68:445–463

Besson M (1975) Les sulfures des lherzolites et ariègites. Bull Soc Fr Mineral Cristallog 98:53–64

Bodinier JL, Guiraud M, Fabries J, Dostal J, Dupuy C (1987a) Petrogenesis of layered pyroxenites from the Lherz, Freychinède and Prades ultramafic bodies (Ariège, French Pyrénées). Geochim Cosmochim Acta 51:279–290

Bodinier JL, Fabries J, Lorand JP, Dostal J, Dupuy C (1987b) Petrogenesis of amphibole pyroxenite veins from the Lherz and Freychinède ultramafic bodies (Ariège, French Pyrenees). Bull Mineral 110:345–359

Bodinier JL, Dupuy G, Dostal J (1988) Petrogenesis and geochemistry of Eastern Pyrenean peridotites. Geochim Cosmochim Acta 52:2893–2952

Cabri LJ (1973) New data on phase relations in the Cu-Fe-S system. Econ Geol 68:443–454

Conquéré F (1971) La lherzolite à amphibole du gisement de Caussou (Ariège, France). Contrib Mineral and Petrol 30:296–313

Conquéré F (1977) Pétrologie des pyroxénites litées dans les complexes ultramafiques de l'Ariège (France). Bull Soc Fr Mineral Cristallog 100:42–80

Conquéré F (1978) Pétrologie des complexes ultramafiques de lherzolite à spinelle de l'Ariège (France). PhD thesis, Paris, pp 333

Conquéré F, Fabries J (1984) Chemical disequilibrium and its thermal significance in spinel peridotites from the Lherz and Freychinède ultramafic bodies (Ariège, French Pyrenees). In: Kornprobst J (ed) The mantle and crust mantle relationships. Proc 3nd Int Kimberlite Conf, vol 2. Elsevier, pp 319–334

Cordellier F (1982) Structures et déformations de massifs ultrabasiques inclus dans le socles Almklovdalen (Norvege) Alpe Arami (Suisse). Theses, Nantes, pp 139

Craig JR (1973) Pyrite-pentlandite assemblages in the Fe-Ni-S system. Am J Sci 273A:496–510

Craig JR, Naldrett AJ (1968) Partial pressure of sulfur in the vapor coexisting with the $Fe_{1-x}S$, $Ni_{1-x}S$ solid solution at 600° and 400° C. Carnegie Inst Washington Yearb 66:436–440

Craig JR, Kullerud G (1969) Phase relations in the Cu-Fe-Ni-S system and their applications to magmatic ore deposits "Magmatic Ore Deposits". Econ Geol, pp 343–358

Dromgoole EL, Pasteris JD (1987) Interpretation of the sulfide assemblages in a suite of xenoliths from Kilbourne Hole, New Mexico. Geol Soc Am Spec Pap 215:25–46

Dutrizac JE (1976) Reactions in cubanite and chalcopyrite. Canad Mineral 14:172–181

Eckstrand OR (1975) The Dumont serpentinite: a model for control of nickeliferous opaque mineral assemblages by alteration reactions in ultramafic rocks. Econ Geol 70:183–201

Ewers WE, Hudson DR (1972) An interpretative study of a nickel-iron sulfide ore intersection, Lunnon Shoot, Kambalda, Western Australia. Econ Geol 76:1075–1092

Fabries J, Conquéré F (1983) Les lherzolites à spinelle et les pyroxénites à grenat associées de Bestiac (Ariège, France). Bull Mineral 106:681–703

Fabries J, Bodinier JL, Dupuy C, Lorand JP, Benkerrou C (1989) Evidence for modal metasomatism in the orogenic spinel lherzolite bodies from Caussou (Northeastern Pyrenees). J Petrol 30:199–229

Garuti G, Gorgoni C, Sighinolfi P (1984) Sulfide mineralogy and chalcophile element abundances in the Ivrea-Verbano mantle peridotites (Western Italian Alps). Earth Planet Sci Lett 70:69–87

Graterol M, Naldrett AJ (1971) Mineralogy of the Marbridge n° 3 and n° 4 nickel iron sulfide deposits with some comments on low-temperature equilibration in the Fe-Ni-S system. Econ Geol 66:886–890

Haggerty SE (1986) Source regions for oxides, sulfides and metal in the upper mantle: clues to the stability of diamonds, and the origin of kimberlites and lamproites. Fourth International Kimberlite Conference, abstract vol, pp 250–252

Hamlyn PR, Keays RR (1986) Sulfur saturation and second-stage melts: application ot the Bushveld platinum metal deposits. Econ Geol 81:1431–1445

Jover O, Rochette P, Lorand JP, Maeder M, Bouchez JL (1989) Magnetic mineralogy of some granites from the French Massif Central. Phys Earth Planet Int 55:79–92

Kaneda H, Takenouchi S, Shoji T (1986) Stability of pentlandite in the Fe-Ni-Co-S system. Mineral Deposit 21:169–181

Kelly DP, Vaughan DJ (1983) Pyrrhotine-pentlandite ore textures: a mechanistic approach. Mineral Mag 47:453–463

Kullerud G, Yoder HS (1959) Pyrite stability in the Fe-S system. Econ Geol 54:534–569

Kullerud G, Yoder HS (1963) Sulfide-silicate reactions. Carnegie Inst Washington Yearb 63:218–222

Kullerud RA, Yund RA, Mohr G (1969) Phase relations in the Cu-Fe-S, Cu-Ni-S and Fe-Ni-S systems, "Magmatic Ore deposits". Econ Geol Monog 4:323–343

Lorand JP (1985) The behaviour of the upper mantle sulfide component during the incipient serpentinization of "alpine"-type peridotites as exemplified by the Beni Bousera (Northern Morocco) and Ronda (Southern Spain) ultramafic bodies. Tsch Mineral Petrol Mitt 34:183–211

Lorand JP (1987) Caractères minéralogiques et chimiques généraux des microphases du système Cu-Fe-Ni-S dans les roches du manteau supérieur: exemples d' hétérogénéités en domaine subcontinental. Bull Soc Geol Fr (8), III:643–657

Lorand JP (1989a) Sulfide petrology of spinel and garnet pyroxenite layers from mantle-derived spinel lherzolite massifs from Ariége (Northeastern Pyrenees, France). J Petrol 30 (in press)

Lorand JP (1989b) The Cu-Fe-Ni sulfide component of the amphibole-rich veins from the Lherz and Freychinède spinel peridotite massifs (Northeastern Pyrenees, France); a comparison with mantle-derived megacrysts from alkali basalts. Lithos 23 (in press)

Lorand JP (1989c) Abundance and distribution of Cu-Fe-Ni sulfides, sulfur, copper and platinum-group elements in orogenic-type spinel peridotites of Ariège (Northeastern Pyrenees, France). Earth Planet Sci Lett 93:50–64

Lorand JP, Conquéré F (1983) Contribution à l'étude des sulfures dans les enclaves de lherzolite à spinelle des basaltes alcalins (Massif Central et Languedoc, France). Bull Mineral 106:585–606

Loubet M, Allègre CJ (1982) Trace elements in orogenic lherzolites reveal the complex history of the upper mantle. Nature 298:809–814

McQueen KG (1979) Experimental heating and diffusion effects in the Fe-Ni-S ore from Redross, Western Australia. Econ Geol 74:140–148

McQueen KG (1981) The nature and metamorphic history of the Wannaway nickel deposit, Western Australia. Econ Geol 76:1444–1468

Mercier JC, Nicolas A (1975) Textures and fabrics of upper mantle peridotites as illustrated by xenoliths from basalts. J Petrol 16:454–487

Misra K, Fleet ME (1973) The chemical composition of synthetic and natural pentlandite assemblages. Econ Geol 68:518–539

Mitchell RH, Keays RR (1981) Abundance and distribution of gold, palladium and iridium in some spinel and garnet lherzolites. Implications for the nature and origin of precious metal-rich intergranular components in the upper mantle. Geochim Cosmochim Acta 45:2425–2445

Moody JB (1976) Serpentinization: a review. Lithos 9:126–138

Naldrett AJ (1969) A portion of the system Fe-S-O between 900° and 1080° C and its applications to sulfide ore magmas. J Petrol 10:171–201

Naldrett AJ, Craig JR, Kullerud G (1967) The central portion of the Fe-Ni-S system and its bearing on pentlandite exsolution in iron-nickel sulfides ores. Econ Geol 62:826–847

Papunen H (1970) Sulfide mineralogy of the Kotalahti and Hitura nickel-copper ores, Finland. Ann Acad Sci Fenn Ser A 109, pp 79

Pasteris JD (1982) Evidence of potassium metasomatism in mantle xenoliths. EOS Trans Am Geophys Union 63:462 (abstract)

Polve M, Allègre CJ (1980) Orogenic lherzolite complexes studied by ^{87}Rb-^{87}Sr: a clue to understand the mantle convection processes? Earth Planet Sci Lett 51:71–93

Roedder E (1984) Fluid inclusions. Rev Mineral 12, pp 644

Reed SJB (1975) Practical correction procedures. In: Woolfson MM, Ziman JM (eds) Electron microprobe analysis. Cambridge University Press, pp 284–287

Ryzhenko BN, Kennedy GC (1973) The effect of pressure on the eutectic in the Fe-FeS system. Am J Sci 273:800–810

Stockman HW, Hlava PF (1984) Platinum-group minerals in Alpine chromitites from Southwestern Oregon. Econ Geol 79:491–508

Takeno S, Moh G, Wang N (1982) Dry mackinawite syntheses. Neues Jahrb Mineral Abh 144:297–301

Toulmin PB, Barton PB (1964) A thermodynamic study of pyrite and pyrrhotite. Geochim Cosmochim Acta 68:641–671

Tsai HM, Shieh YN, Meyer HOA (1979) Mineralogy and $^{34}S/^{32}S$ ratios of sulfides associated with kimberlites, xenoliths and diamonds. In: Boyd FR, Meyer HOA (eds) The mantle sample; inclusions in kimberlites and other volcanics. Proc 2nd Int Kimberlite Conf, vol 2. Washington, AGU, pp 87–103

Vaughan D, Craig JR (1978) Mineral chemistry of metal sulfides. In: Harland WB, Cook AH, Hughes NF (eds) Cambridge Univ Press, pp 439

Vétil JY, Lorand JP, Fabries J (1988) Conditions de mise en place des filons de pyroxenites à amphibole du massif ultramafique de Lherz (Ariège, France). C R Acad Sci 307 (Ser II):587–593

Wattmuff IG (1974) Supergene alteration of the Mt Windarra nickel sulphide ore deposits, Western Australia. Mineral Deposit 9:199–221

Wendlandt RF (1982) Sulfur saturation of basalt and andesite melts at high pressure and temperature. Am Mineral 67: 877–895

Yund RA, Hall HT (1970) Kinetics and mechanism of pyrite exsolution from pyrrhotite. J Petrol 11:381–404

Received December 14, 1988 / Accepted August 1, 1989
Editoridal responsibility: R. Binns